Society of Medical Education & Research

2024, Volume 4, Issue 2, Page No: 81-95
ISSN: 3108-4834

Archive of International Journal of Cancer and Allied Science

CTCF-Mediated Insulator Dynamics Reprogram MMP Gene Expression Driving Aggressive Breast Cancer Invasion

Patrick Aidan Murphy[1], Ciara Louise Nolan[1]*, Brian Thomas Walsh[2], Kevin Michael Doyle[2], Declan Seamus Ryan[3], Eoin Patrick Brennan[3]

[1]Trinity Translational Cancer Research Centre, Dublin, Ireland.
[2]Department of Oncology, Royal College of Surgeons in Ireland, Dublin, Ireland.
[3]National Cancer Control Programme, Health Service Executive, Dublin, Ireland.

***E-mail** ✉ c.nolan.tcd@gmail.com

Abstract

Triple-negative breast cancer (TNBC) is a highly aggressive form of breast cancer, marked by frequent metastasis and limited targeted therapies. The mechanisms by which epigenomic regulation influences matrix metalloprotease (MMP) activity—and thereby tumor invasiveness—remain incompletely understood. We integrated transcriptomic and chromatin conformation datasets to identify candidate insulator elements that might coordinate MMP gene expression and invasive potential. Using CRISPR/Cas9, we specifically disrupted a CTCF binding site within an insulator element downstream of MMP8 (IE8) in two TNBC cell models. The resulting cells were profiled through Hi-C, ATAC-seq, and RNA-seq, alongside functional assays to assess invasion. We also evaluated the prognostic relevance of these regulatory elements in clinical ductal carcinoma in situ (DCIS) samples. We characterized a functional insulator at the Chr11q22.2 locus (IE8) that establishes a TAD boundary, partitioning nine MMP genes into two inversely regulated clusters. This MMP expression architecture was linked to shorter relapse-free (HR = 1.57 [1.06–2.33]; p = 0.023) and overall survival (HR = 2.65 [1.31–5.37]; p = 0.005) in TNBC patients. CRISPR-mediated IE8 disruption reshaped the MMP expression landscape, suppressing the pro-invasive MMP1 while inducing the anti-tumorigenic MMP8, leading to reduced invasion and collagen degradation. Furthermore, this MMP signature predicted DCIS progression to invasive carcinoma (AUC = 0.77, p < 0.01). Our study reveals that a single insulator element near MMP8 orchestrates the regional regulation of MMP genes with opposing roles, directly impacting the invasive behavior of aggressive breast cancers.

Keywords: MMP1, MMP8, CTCF, Insulator, Chromatin architecture, Gene regulation, Breast cancer, Invasion, ATAC-seq, RNA-seq, Hi-C

Introduction

Breast cancer remains the leading cause of cancer-related mortality among women [1], with 20–30% of early-stage patients eventually developing distant metastases [2]. Disease aggressiveness varies across subtypes; notably, triple-negative breast cancer (TNBC), characterized by the absence of estrogen and progesterone receptors and lack of HER2 amplification [3], exhibits poorer survival outcomes and higher rates of lung, brain, and distant nodal metastases than other subtypes [2]. Tumor invasion—the ability to penetrate surrounding tissues and establish secondary lesions—accounts for the majority of cancer-related deaths [4]. Clinically, invasion is critical not only in metastasis but also in the transition of ductal carcinoma in situ (DCIS) to invasive ductal carcinoma (IDC), a process that remains a significant therapeutic challenge [5].

Incomplete understanding of the molecular mechanisms underlying invasion contributes to overtreatment in early

Access this article online https://smerpub.com/

Received: 21 April 2024; **Accepted:** 28 August 2024

How to cite this article: Murphy PA, Nolan CL, Walsh BT, Doyle KM, Ryan DS, Brennan EP. CTCF-Mediated Insulator Dynamics Reprogram MMP Gene Expression Driving Aggressive Breast Cancer Invasion. Arch Int J Cancer Allied Sci. 2024;4(2):81-95. https://doi.org/10.51847/IjUQf9AsYu

breast cancer and limits strategies to prevent metastasis [6]. Both local invasion and distant metastasis are orchestrated by tightly regulated gene expression programs. Matrix metalloproteinases (MMPs) are central mediators of this process [7], remodeling the extracellular matrix (ECM) and facilitating the release of cytokines and growth factors that drive angiogenesis, epithelial-to-mesenchymal transition (EMT), and inflammatory responses [8]. The human MMP family includes 23 proteolytic enzymes, either secreted or cell surface-bound [9], whose spatiotemporal regulation is frequently lost during tumorigenesis [10]. Upregulation of MMP1, MMP2, and MMP9 has been linked to poor prognosis across multiple cancers, including breast cancer [11–13]. Interestingly, not all MMPs act as tumor promoters; for instance, MMP8, although associated with worse outcomes in liver and gastric cancers, appears to inhibit metastasis in head and neck, skin, and breast cancers [14–16]. These findings challenge the conventional view that MMPs uniformly drive tumor progression, highlighting the need to better understand their context-dependent roles [17].

Aberrant MMP expression in cancer often involves epigenetic mechanisms. At least 14 MMP genes contain CpG islands in their promoters, where DNA methylation can suppress expression [18]. Inhibition of DNA methyltransferases with agents like 5-aza-2′-deoxycytidine can restore MMP2 and MMP9 expression in pancreatic and breast cancer cells, respectively [19, 20]. Beyond promoter methylation, higher-order chromatin structure also influences transcription by modulating regulatory elements such as enhancers and insulators.

In this study, we investigated the regulatory landscape of a genomic locus on Chr11q22.2 containing nine MMP genes. By combining multi-omics profiling with functional assays, we demonstrate that disruption of an insulator element near MMP8 reshapes local chromatin architecture, alters promoter accessibility, and reprograms gene expression. Specifically, impairment of this insulator decreases the pro-invasive MMP1 while increasing MMP8, a combination associated with antitumor effects in breast cancer. Functionally, these changes reduce invasiveness in cellular models. Moreover, tumors can be stratified based on the balance between pro-invasive and antitumor MMP expression near the MMP8 insulator, a signature correlated with disease-free and overall survival in invasive TNBC and predictive of DCIS progression to IDC. Collectively, these findings reveal a regional regulatory role for a chromatin insulator in MMP expression reprogramming, contributing to the invasive potential of aggressive breast cancers.

Materials and Methods

Data acquisition and processing

We accessed mRNA expression and clinical datasets from The Cancer Genome Atlas (TCGA) using the TCGAbiolinks R package. Patients were filtered to include only triple-negative breast cancer (TNBC) cases, defined by the absence of estrogen and progesterone receptors and HER2 amplification [21, 22]. Only samples with a tumor purity above 66%, as calculated per Aran *et al*. [23], were retained. Long-range chromatin interaction data were retrieved from ChIA-PET experiments and visualized via the WashU Epigenome Browser [24]. Survival analyses were performed with the KM plotter platform [25] using gene chip breast cancer datasets, with TNBC defined as ER- and HER2-negative. Follow-up was capped at 60 months, and Kaplan–Meier curves were generated as of July 6, 2022. Expression quantitative trait loci (eQTLs) for MMPs within Chr11q22.2 were downloaded from GTEx [26], with arcs representing SNP positions relative to the transcription start sites of target genes. Arc height indicated significance, while direction corresponded to whether the SNP increased or decreased expression. Gene expression data for breast cancer cell lines were obtained from CCLE DepMap 22Q2 Primary Files [27]. Non-coding mutations in the Chr11q22.2 locus were evaluated using the PCAWAG consensus SNV/Indel callset (N = 2,658) [28] and whole-genome sequences from 237 TNBC samples [29]. Data visualization and analysis were conducted using R packages including corrplot, ggbio, ggpubr, patchwork, pheatmap, rstatix, RColorBrewer, tidyverse, and viridis.

Cell culture

MDA-MB-231 and MDA-MB-436 cell lines were sourced from ATCC and maintained in RPMI 1640 Glutamax™ medium supplemented with 10% fetal bovine serum and 1% penicillin/streptomycin under standard conditions (37 °C, 5% CO_2). Cell line identity was verified by short tandem repeat profiling (Genetics Core, University of Arizona, Phoenix, USA), and all cultures were periodically screened for mycoplasma contamination using the MycoAlert Mycoplasma Detection Kit (Lonza).

Clinical tissue profiling

Gene expression in invasive and in situ breast cancer tissues was examined using the SCAN-B cohort [30, 31]. Samples lacking tumor size, relapse data, or with follow-up under three years were excluded. Relapse-free survival was used as the primary endpoint. Raw read counts were normalized via $\log_2$(Counts + 1), and each MMP gene's expression was standardized to the cohort median. Undetectable signals were substituted with the minimal detected value for the respective gene. The cohort comprised 85 DCIS samples (14 progressing to IDC) and 3,620 invasive ductal carcinomas stratified by tumor size (T1: n = 2,558; T2: n = 1,006; T3: n = 56). Kaplan–Meier survival curves and receiver operating characteristic analyses were conducted with pROC v1.16.2. MMP expression was further validated in the TBCRC 038 cohort, which included DCIS patients with (n = 121) or without (n = 95) subsequent ipsilateral breast events [32]. Differential gene expression between these groups was analyzed to evaluate MMP regulation.

Additional experimental procedures

Extended methodological details include generation of experimental models (IE8 disruption and ectopic hMMP1/MMP1mut expression), analysis of copy number variations and cell-type composition, CUT&RUN, qPCR, and multi-omics assays (Hi-C, ATAC-seq, RNA-seq). Protein quantification of MMP1 and MMP8, along with functional assays such as fatty acid uptake, MMP1 enzymatic activity, proliferation, colony formation, wound healing, collagen I degradation, anchorage-independent growth, and collagen-based invasion assays, are described in the supplementary methods.

Results and Discussion

MMP expression alterations correlate with relapse-free and overall survival

Considering the central role of MMPs in initiating metastasis, we first compared mRNA expression levels between TNBC tumors and normal breast tissue using The Cancer Genome Atlas (TCGA) cohort. Among TNBC tumors (n = 90) relative to normal samples (n = 99), seven MMP genes were significantly downregulated, whereas ten were upregulated (Figure S1a). Notably, six of the upregulated MMPs are consecutively encoded within the same genomic locus, Chr11q22.2, which contains a total of nine MMP genes; **(Figure 1a).**

Analysis of coexpression patterns across this locus revealed two distinct clusters in TNBC tumors. The 5′ cluster comprises MMP7, MMP8, MMP20, and MMP27, along with neighboring non-MMP genes TMEM123 and BIRC3. The 3′ cluster includes MMP1, MMP3, MMP10, MMP12, and MMP13 **(Figure 1b).** When evaluating the relative expression between these clusters, the ratio of 3′ to 5′ MMP expression (3′MMPs/5′MMPs) was significantly elevated in TNBC samples compared to normal tissue, suggesting coordinated dysregulation of this locus in aggressive tumors.

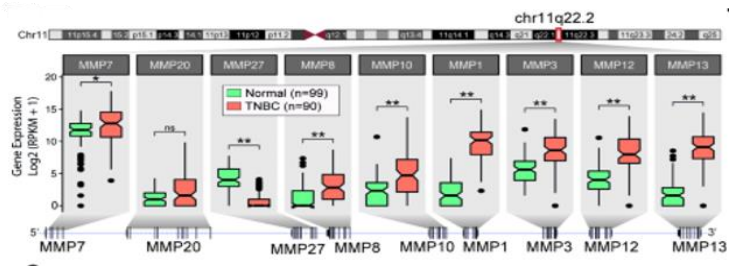

a)

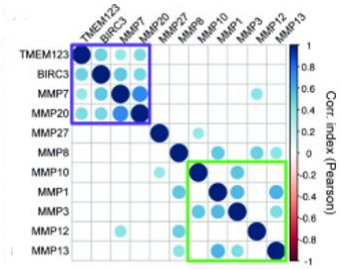

b)

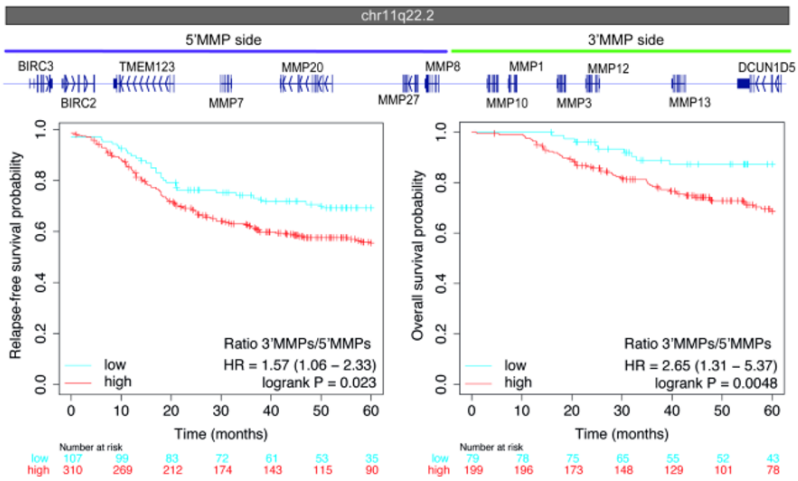

c)

Figure 1. mRNA expression in TNBC tumors

MMP expression patterns are linked to clinical outcomes in TNBC

To investigate the role of MMPs in early metastatic events, we first analyzed mRNA expression in TNBC tumors (n = 90) versus normal breast tissues (n = 99) from the TCGA cohort. This analysis revealed seven MMPs significantly downregulated and ten upregulated in TNBC. Remarkably, six consecutively upregulated MMPs are encoded within a single genomic locus at Chr11q22.2, which harbors a total of nine MMP genes; **(Figure 1a).**

Coexpression analyses within this locus identified two distinct expression clusters. The 5′ cluster includes MMP7, MMP8, MMP20, and MMP27, alongside neighboring non-MMP genes TMEM123 and BIRC3. The 3′ cluster comprises MMP1, MMP3, MMP10, MMP12, and MMP13 **(Figure 1b).** TNBC tumors exhibited a significantly higher ratio of 3′ to 5′ MMP expression (3′MMPs/5′MMPs) compared to normal tissue.

To determine whether these differences were influenced by chromosomal alterations, we examined copy number variations (CNVs). Although TNBC and HER2-positive tumors exhibited more CNAs compared to hormone receptor-positive (HR+) cancers, these changes did not correlate with MMP locus expression. We also assessed tumor heterogeneity using transcriptome deconvolution [33] and found that MMP signatures showed minimal correlation with stromal content. The 5′ and 3′ MMP clusters exhibited weak correlations with immune infiltration (r = 0.23 and 0.27, respectively) and total tumor microenvironment content (r = 0.26 and 0.33, respectively), while the 3′/5′ MMP ratio was independent of these variables.

Next, we evaluated clinical relevance. In TNBC patients (n = 417), a higher 3′/5′ MMP ratio was associated with significantly shorter relapse-free survival (RFS; log-rank P = 0.023; HR = 1.57, 95% CI 1.06–2.33) and overall survival (OS; log-rank P = 0.005; HR = 2.65, 95% CI 1.31–5.37) **(Figure 1c).** When considered separately, high 5′ MMP expression correlated with improved RFS and OS, whereas 3′ MMP expression alone did not show prognostic significance. Similar trends were observed in hormone receptor-positive breast cancers, while the ratio had no impact in HER2-positive cases. Interestingly, this signature was prognostic in other solid tumors: it predicted worse outcomes in liver cancer, lung adenocarcinoma, and sarcoma, but was associated with better survival in gastric cancer.

An insulator element near MMP8 influences regional MMP regulation

Given the clustered expression patterns at Chr11q22.2, we mapped regulatory elements within this locus. We identified 29 putative insulator elements (IEs) and 13 potential enhancers (EEs) **(Figure 2a).** Insulators, which are bound by CCCTC-binding factor (CTCF), play critical roles in establishing topologically associating domains (TADs) and chromatin loops [34]. Using CTCF ChIA-PET data, we identified a candidate TAD boundary

located between the MMP8 promoter and MMP10 gene body (Chr11:102,732,800–102,733,900, hg38), hereafter referred to as IE8. IE8 appears to segregate the 5′ and 3′ MMP clusters, consistent with the observed coexpression patterns. Supporting this, eQTL analyses revealed that SNPs preferentially modulate genes within the same TAD at this locus. Notably, the CTCF binding site of IE8 showed very low mutation frequency across 2,658 tumors in PCAWAG and 237 TNBC whole-genome sequences, suggesting that intact IE8 function is preserved and potentially required for tumor biology.

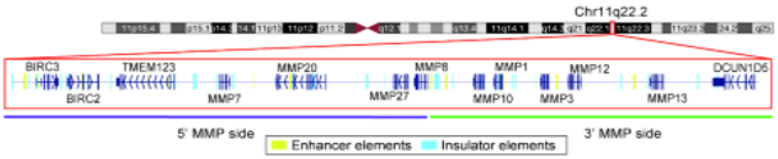

a)

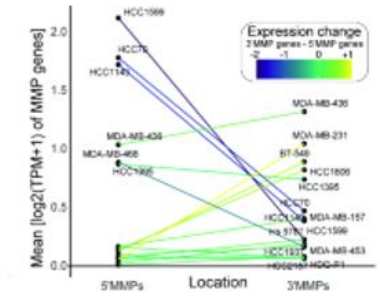

b)

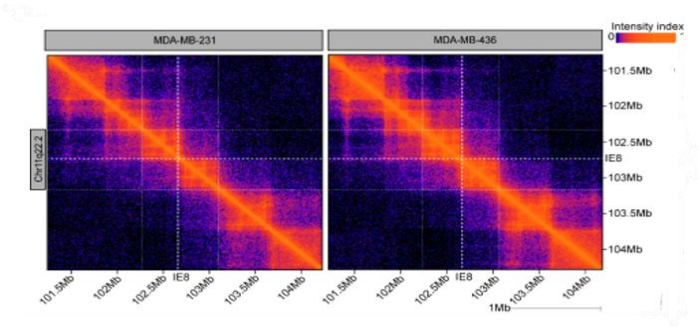

c)

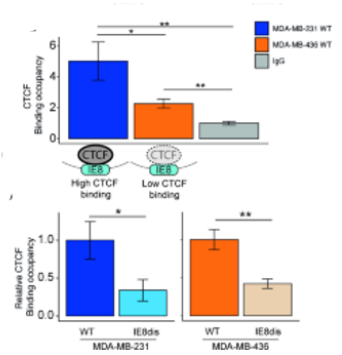

d)

Figure 2. Identification and editing of gene regulatory elements at chr11q22.2.

a. Schematic representation of the identified enhancer and insulator elements, with the CRISPR/Cas9-targeted Insulator Element 8 (IE8) highlighted.

b. Expression profiles of 5’ and 3’ MMP genes in TNBC cell lines.

c. Hi-C contact frequency matrix for a 3 Mb genomic region surrounding IE8 at 10-kb resolution.
d. CTCF binding shown as fold enrichment relative to isotype control in MDA-MB-231 and MDA-MB-436 (top), and fold change after IE8 disruption (bottom). Statistical significance determined by Student's t-test: *P < 0.05, **P < 0.01.

Establishment of cell models to study IE8's effect on MMP gene expression

To select TNBC cell models reflecting clinical expression patterns, patients were stratified based on their 3'MMP/5'MMP ratios into high, intermediate, and normal-like groups. Subsequently, MMP gene expression was profiled in 17 well-characterized TNBC cell lines **(Figure 2b)**, leading to the selection of two representative lines: MDA-MB-231 (high 3'MMP/5'MMP) and MDA-MB-436 (intermediate 3'MMP/5'MMP). Hi-C analysis revealed that IE8 colocalizes with TAD boundaries in both lines, suggesting an active insulator function **(Figure 2c),** consistent with ChIA-PET data.

Both cell lines were transiently transfected with a Cas9 plasmid and a sgRNA to stably disrupt the CTCF-binding motif of IE8 using CRISPR/Cas9. Single clones were isolated for downstream analyses. CUT&RUN followed by qPCR showed that basal CTCF occupancy at IE8 was higher in MDA-MB-231 than in MDA-MB-436, reflecting variability observed in clinical samples. IE8 disruption significantly reduced CTCF binding in both lines **(Figure 2d).**

Hi-C performed post-IE8 disruption showed no major changes in overall TAD organization. However, IE8 was found to interact with distal 3'MMP regulatory regions, often with other insulator elements in convergent orientation—a requirement for IE-mediated interactions [35]. This indicates that IE8-mediated insulation predominantly affects the 3'MMP region of the chr11q22.2 locus. High-confidence interchromosomal interactions were also detected, linking the MMP locus ends to super-enhancers on other chromosomes.

IE8 disruption alters local chromatin accessibility

To examine the effect of IE8 disruption on chromatin accessibility, ATAC-seq was conducted. MDA-MB-231 showed 34,047 common peaks, and MDA-MB-436 had 35,347. Differential accessibility was assessed based on peaks unique to one condition (WT or IE8-disrupted) or significant changes in shared peaks. In MDA-MB-231, 3,083 regions gained and 2,232 lost accessibility post-IE8 disruption. In MDA-MB-436, 8,673 regions became more accessible and 370 less accessible **(Figure 3a).** Notably, 1,033 regions overlapped between both models, highlighting shared chromatin changes.

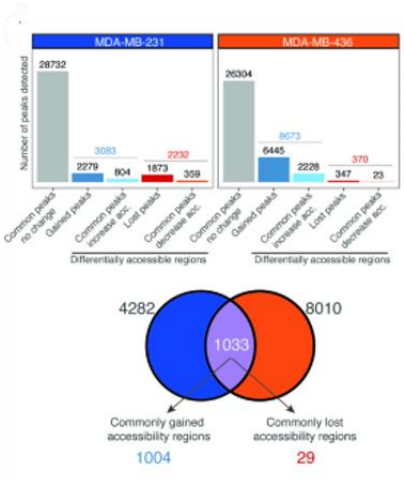

a)

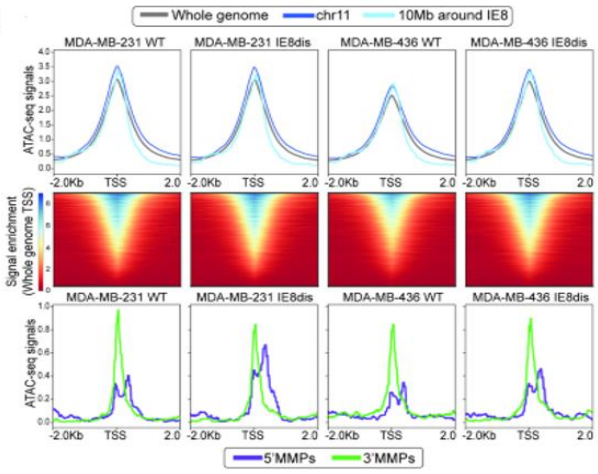

b)

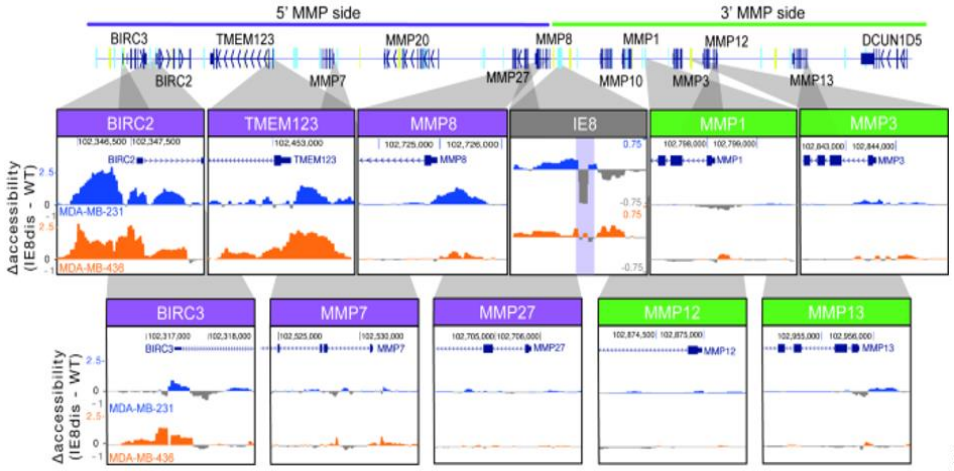

Figure 3. Local effects of IE8 disruption.

a. (Top) Overview of differentially accessible regions (DARs) in MDA-MB-231 and MDA-MB-436 following IE8 disruption; (Bottom) representation of regions commonly altered in both cell lines.

b. (Top) ATAC-seq peak intensity across all TSS in the genome, on chromosome 11, and within a 10 Mb region surrounding IE8; (Middle) heatmap of active TSS in TNBC models; (Bottom) changes in promoter accessibility for 5' MMPs (purple) and 3' MMPs (green) in MDA-MB-231 and MDA-MB-436 before and after IE8 disruption.

c. Representative examples of accessibility changes upon IE8 disruption (IE8-dis minus WT) in the IE8 region (gray), 5' MMP region (purple), and 3' MMP region (green).

Although chromatin accessibility changes were observed genome-wide, we investigated whether these alterations were enriched near IE8. Differentially accessible regions on chromosome 11, as well as within windows of varying sizes around IE8 (±0.5–10 Mb), were analyzed. A significant enrichment of DARs was detected in the immediate vicinity of IE8, while no notable differences were seen across the rest of chromosome 11.

Next, we aimed to identify regulatory elements associated with these accessibility changes. The proportions of promoters, enhancers, and insulators showing differential accessibility after IE8 disruption were similar between MDA-MB-231 and MDA-MB-436. Focusing on ±2 kb around transcription start sites (TSS), heatmaps revealed comparable accessibility profiles across conditions, with peak enrichment at TSS **(Figure 3b)**. Similar patterns were observed when centering peaks on enhancers and insulators.

However, interesting differences emerged at the Chr11q22.2 locus. Promoters in the 5' MMP region

exhibited increased accessibility following IE8 disruption, while promoters in the 3' MMP region remained largely unchanged **(Figures 3b-3c)**. Enhancer accessibility was altered in both 5' and 3' MMP regions. Additionally, chromatin accessibility at the IE8 CTCF-binding site targeted by CRISPR/Cas9 decreased, particularly in MDA-MB-231 cells, consistent with higher baseline CTCF occupancy observed via CUT&RUN **(Figure 2d).**

IE8 disruption affects regional MMP gene expression

To determine whether these chromatin accessibility changes translated into transcriptional effects, RNA-seq was performed in wild-type and IE8-disrupted cells. A total of 237 mRNAs were significantly differentially expressed upon IE8 disruption **(Figure 4a),** including 166 upregulated and 71 downregulated genes. Gene ontology (GO) analysis revealed enrichment for extracellular matrix organization and Ca^{2+}-dependent cell-cell adhesion. Additionally, fatty acid import pathways were upregulated, a feature associated with favorable prognosis in TNBC [36]. Functionally, both cell lines exhibited increased fatty acid uptake following IE8 disruption.

Because IE8 is located on chromosome 11, we assessed whether expression changes were enriched in this region. No significant genome-wide changes were observed, but genes within 1 Mb of IE8 were significantly modulated in MDA-MB-231 cells **(Figure 4b),** highlighting the local regulatory impact of IE8 disruption.

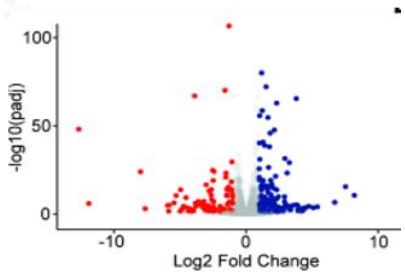

a)

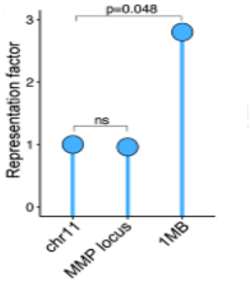

b)

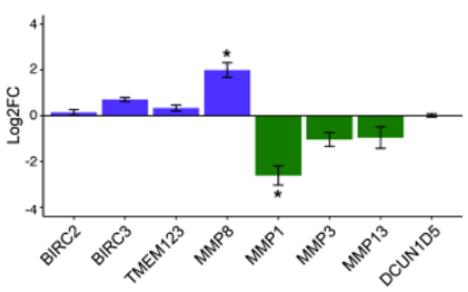

c)

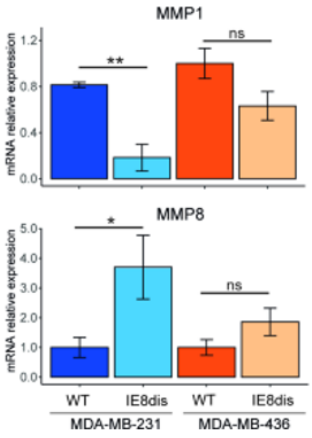

d)

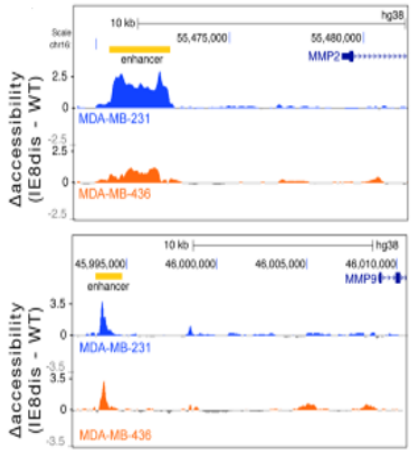

e)

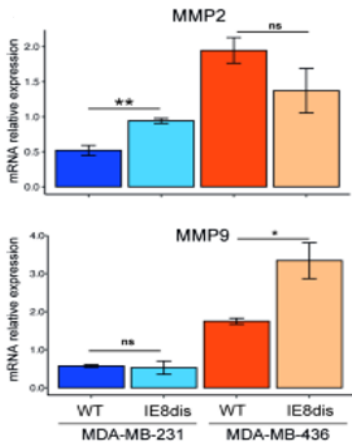

f)

Figure 4. Impact of IE8 disruption on MMP gene expression and chromatin accessibility.

Analysis of the Chr11q22.2 locus demonstrated that changes in chromatin accessibility translated into local transcriptional effects. RNA-seq in MDA-MB-231 revealed that IE8 disruption led to upregulation of MMP8 and downregulation of MMP1 **(Figure 4c),** a pattern validated by qPCR in both MDA-MB-231 and MDA-MB-436 **(Figure 4d).** In MDA-MB-231, this shift reduced the abundance of the pro-invasive MMP1 while enhancing MMP8, which is associated with tumor-suppressive activity, effectively lowering the MMP1/MMP8 ratio to levels similar to normal breast tissue. Although MDA-MB-436 showed similar trends, the changes did not reach statistical significance. Notably, these expression changes occurred independently of interchromosomal contacts.

To investigate potential compensatory mechanisms, we examined the expression of TIMP family members (TIMP1–4), which regulate MMP activity, as well as other metalloproteinases MMP2 and MMP9. TIMP expression remained unchanged after IE8 disruption (Figure S8d). While promoter accessibility at MMP2 and MMP9 was unaffected, upstream enhancer regions exhibited increased accessibility (8 kb upstream of MMP2 and 15 kb upstream of MMP9); **(Figure 4e).** This correlated with selective upregulation of MMP2 in MDA-MB-231 and MMP9 in MDA-MB-436 **(Figure 4f)**, highlighting a cell line-specific enhancer-mediated effect.

We next compared these observations to TNBC patient samples from TCGA with matched ATAC-seq and RNA-seq data. Accessibility at IE8 varied across the six samples examined, and higher IE8 accessibility strongly correlated with an elevated 3'MMP/5'MMP expression ratio (r = 0.87, p = 0.02; Figure S8f), supporting the relevance of our in vitro findings in clinical tumors.

Functional consequences of IE8 disruption on protein levels and invasion

Consistent with transcriptional changes, IE8 deletion increased MMP8 protein levels while reducing MMP1 abundance and activity in both TNBC models **(Figures 5a-5c).** IE8 disruption did not affect proliferation, clonogenicity, or wound healing capacity. However, MDA-MB-231 cells showed impaired degradation of collagen type I, a major ECM component, whereas MDA-MB-436 remained unaffected. Anchorage-independent growth was also reduced in IE8-depleted MDA-MB-231 cells, with no effect in MDA-MB-436 **(Figure 5d)**. Importantly, invasion assays on collagen I confirmed that IE8 loss reduced invasive behavior in both cell lines **(Figure 5e).**

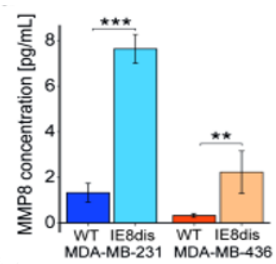

a)

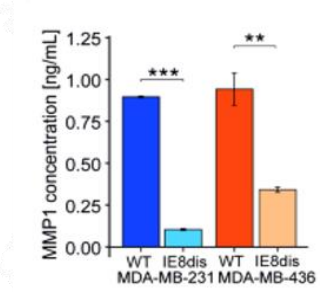

b)

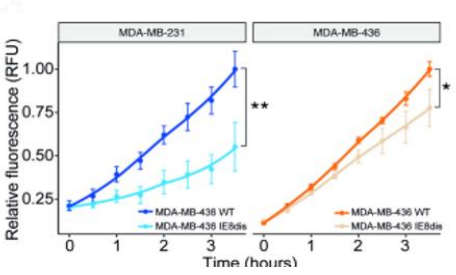

c)

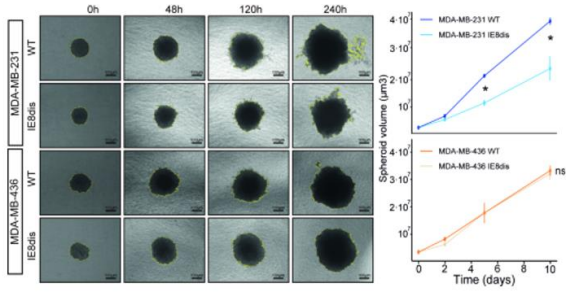

d)

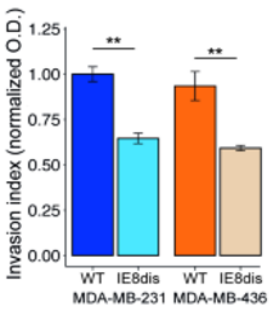

e)

Figure 5. Functional consequences of IE8-mediated changes in MMP expression and activity.

a-b. Extracellular levels of MMP8 and MMP1 were assessed in MDA-MB-231 and MDA-MB-436 cells after IE8 disruption.

c. Time-course analysis of MMP1 enzymatic activity in both cell lines following IE8 loss.

d. Left: representative images of anchorage-independent spheroid growth; right: quantification of spheroid volume.

e. Colorimetric measurement of invasive capacity on collagen I-coated membranes. Statistical significance was determined using Student's t-test (ns = not significant, *P < 0.05, **P < 0.01, ***P < 0.001).

To test whether the observed functional changes could be reversed, IE8-disrupted MDA-MB-231 and MDA-MB-436 cells were transfected with either a catalytically active MMP1 (hMMP1) or an inactive mutant form (MMP1mut). Both constructs successfully elevated MMP1 mRNA levels, but only hMMP1 increased enzymatic activity. Functional assays showed that neither construct affected cell proliferation. However, hMMP1 expression restored clonogenic growth and accelerated wound closure, while MMP1mut had no effect. Furthermore, active MMP1 overexpression in IE8-disrupted cells enhanced invasive capacity through collagen I-coated membranes. These results indicate that IE8 disruption limits invasion in collagen-rich environments primarily by reprogramming the local MMP expression landscape.

MMP expression dynamics predict progression from DCIS to invasive breast cancer

To investigate clinical relevance, we analyzed transcriptomic and clinicopathological data from the SCAN-B cohort [30], comparing normal breast tissue, ductal carcinoma in situ (DCIS), and invasive ductal carcinoma (IDC) across different TNM stages. The 3'MMP/5'MMP ratio was significantly elevated in DCIS and IDC relative to normal tissue (PDCIS < 0.001, PIDC < 0.001). Notably, DCIS lesions that progressed to invasive disease exhibited higher MMP ratios than non-progressing DCIS **(Figure 6a).** Considering the ratio of pro-invasive MMP1 to antimetastatic MMP8, the difference was even more pronounced in progressing DCIS (P = 0.002); **(Figure 6b).** High MMP ratios were also associated with shorter relapse-free survival in DCIS patients (p < 0.001); **(Figures 6c-6d).**

Receiver operating characteristic (ROC) analysis demonstrated that both the 3'MMP/5'MMP and MMP1/MMP8 ratios effectively predicted progression from DCIS to invasive disease (AUC 0.67 and 0.77, respectively); (Figure 6e-6f), whereas individual 3'MMP or 5'MMP signatures lacked predictive power. Finally, in an independent DCIS cohort from the TBCRC 038 clinical trial [32], MMP1 expression was significantly higher in lesions from patients who experienced ipsilateral breast events, further supporting the association of MMP shifts with early tumor progression.

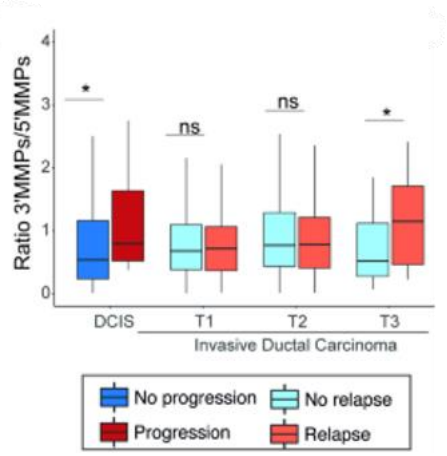

a)

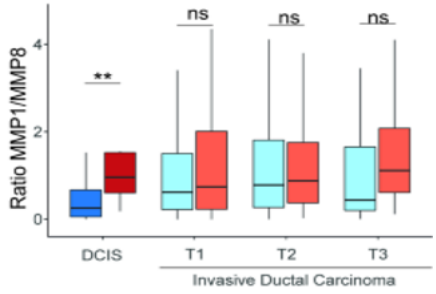

b)

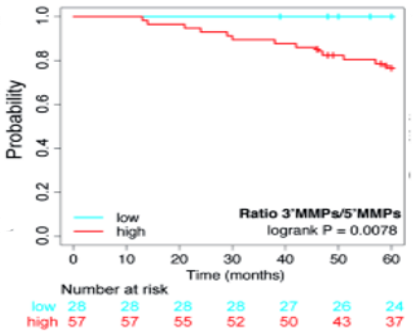

c)

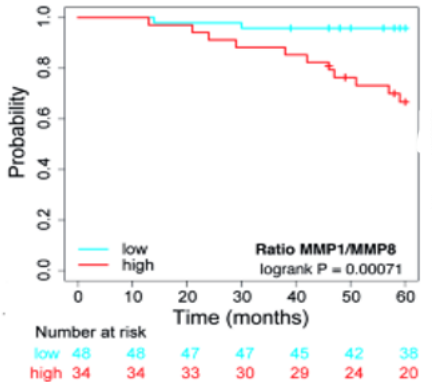

d)

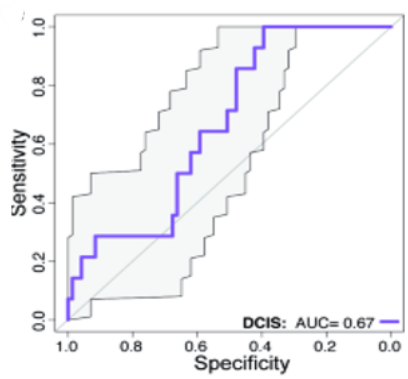

e)

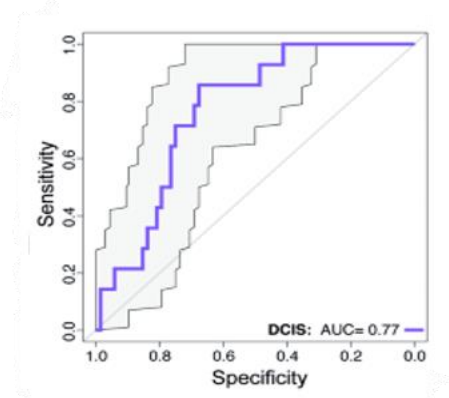

f)

Figure 6. MMP expression ratios and DCIS progression.

a-b. Ratios of 3'MMPs/5'MMPs and MMP1/MMP8 in DCIS and invasive ductal carcinoma (IDC) show that both metrics are significantly elevated in lesions compared to normal breast tissue (Mann-Whitney test, $P < 0.01$).

c-d. Kaplan-Meier analysis indicates that higher 3'MMP/5'MMP and MMP1/MMP8 ratios are associated with shorter relapse-free survival in DCIS patients.

e-f. ROC curves demonstrate the predictive performance of these ratios for DCIS progression to invasive disease.

Metastasis is a multistep process that begins with the detachment of tumor cells from their primary niche and culminates in colonization of secondary sites. In early stages, cancer cells degrade the basement membrane via MMPs and undergo epithelial-to-mesenchymal transition, engaging in dynamic interactions with stromal components [37]. Our study identifies a regulatory insulator element near MMP8 (IE8) that orchestrates the expression of nine MMP genes at the Chr11q22.2 locus. Disruption of IE8 using CRISPR/Cas9 altered local chromatin accessibility and transcriptional profiles, leading to increased MMP8 and decreased MMP1 expression. These molecular changes were mirrored at the protein level and significantly influenced the invasive behavior of TNBC cells.

MMP1 is well-established as a pro-metastatic factor in multiple cancers, including TNBC [38]. Previous studies show that MMP1 overexpression promotes lymph node metastasis in xenograft models and is enriched in exosomes from metastatic TNBC patients [39]. RUNX2-driven MMP1 upregulation has also been linked to

chemoresistance [40]. In TNBC, MMP1 knockdown reduces proliferation, migration, and colony formation [12], yet IE8 disruption did not produce comparable effects, likely because the reduction in MMP1 expression was moderate compared to targeted shRNA approaches. Additionally, the observed cell line-specific increases in MMP2 and MMP9 may buffer the effects of lower MMP1, highlighting a complex interplay between MMP family members. The observed reduction in invasion after IE8 loss aligns with findings from Lim *et al*., who reported similar effects following knockdown of the MMP1 activator YBX1 [41].

The role of MMP8 in cancer is context-dependent, but in breast cancer, it generally appears protective. MMP8 overexpression decreases invasiveness in vitro [42], reduces tumor growth in mouse models [43], and correlates with lower lymph node metastasis rates [14]. Mechanistically, MMP8 can cleave decorin, suppress TGF-β signaling, downregulate miR-21, and induce tumor suppressors such as PDCD4 [44]. It also influences ECM remodeling, promoting cell-cell adhesion [45] and modulating activity of other MMPs, including MMP3. Our data suggest that differential CTCF occupancy at IE8 may coordinate a compensatory balance among Chr11q22.2 MMPs, whereby activation of MMP8 and 5'MMP genes coincides with suppression of MMP1 and other 3'MMP genes, collectively limiting invasiveness.

Overall, these findings emphasize the importance of evaluating the entire MMP locus at Chr11q22.2 rather than individual genes when assessing breast cancer progression risk. Understanding the integrated regulatory network of MMPs may also inform therapeutic strategies targeting tumor invasion and metastasis.

Analysis of patient samples revealed that the ratios of 3'MMPs/5'MMPs and MMP1/MMP8 were elevated in DCIS lesions that eventually progressed to invasive disease **(Figure 6)**. Previous studies have linked MMP1 upregulation with DCIS exhibiting micro-invasive foci [46], whereas loss of MMP8 has been associated with disease progression [45]. Notably, the MMP1/MMP8 ratio alone performed comparably to the HTAN DCIS classifier developed by Strand *et al*. [32] in the TBCRC 038 cohort (AUC = 0.72 in the RAHBT validation cohort), suggesting that this shift in MMP balance is a relevant molecular feature during the transition to invasiveness. While further studies are necessary to clarify the role of IE8 activation in breast cancer invasion, these findings highlight a potential dynamic regulation of the Chr11q22.2 locus during disease progression.

Genome-wide analyses have consistently shown that chromatin loops frequently coincide with CTCF binding sites [47]. Perturbation of these sites—through deletion or inversion—can disrupt chromatin architecture and disturb promoter-enhancer communication [48, 49], and cancer-specific gains or losses of CTCF binding contribute to oncogenic transcriptional programs [50]. CTCF binding can be altered not only by somatic mutations [51] but also through DNA methylation [52]. In our TNBC models, CTCF robustly occupies the IE8 site. Following IE8 disruption and CTCF decoupling, previously insulated regulatory elements in both the 5' and 3' MMP regions become physically accessible, resulting in increased promoter accessibility in the 5'MMP cluster and enhanced exposure of distal enhancers in both clusters. This regulatory relationship is not limited to cell models: in TNBC patient samples, chromatin accessibility at IE8 strongly correlates with the 3'MMP/5'MMP expression ratio, supporting a key role for IE8 in modulating gene expression at Chr11q22.2.

Conclusion

In conclusion, by integrating multi-omics profiling with functional assays, we demonstrate that a single chromatin insulator positioned between MMP8 and MMP10 orchestrates the coordinated expression of two MMP gene clusters in TNBC. This regulation influences invasiveness and appears to impact both DCIS progression and patient survival, highlighting IE8 as a potential node for therapeutic intervention in breast cancer.

Acknowledgments: This project was supported by the National Genomics Infrastructure in Stockholm funded by Science for Life Laboratory, the Knut and Alice Wallenberg Foundation and the Swedish Research Council, and SNIC/Uppsala Multidisciplinary Center for Advanced Computational Science for assistance with massively parallel sequencing and access to the UPPMAX computational infrastructure. We also want to acknowledge Llabata. P, Pellicer. B and Pierola J. for their technical support in RNA-seq, CUT&RUN, and Cell imaging experiments, respectively.

Conflict of Interest: None

Financial Support: This work was supported by the Instituto de la Salud Carlos III (ISCIII) Sara Borrell project (#CD22/00026), Miguel Servet Project (#CPII22/00004), and AES 2022 (#PI22/01496) co-funded by European Union, the Institut d'Investigació Sanitària Illes Balears (FOLIUM program, García-Palmer program, Llavor program and IMPETUS Call IMP21/10), the Govern de les Illes Balears (Margalida Comas program), the Fundación Francisco Cobos, the Asociación Española Contra el Cancer (AECC), the department of European Funds, University, and Culture of the Government of the Balearic Islands and the "CONTIGO Contra el Cancer de Mujer" foundation (#MERIT project). The Fashion Footwear Association of New York (FFANY) Foundation. The group acknowledges support from the EASI-Genomics project, which has received funding from the European Union's Horizon 2020 research and innovation program under grant agreement No 824110.

Ethics Statement: This study was approved by the Institutional Research Board of Hospital Universitario Son Espases (Code CI-542-21). It was performed following the Declaration of Helsinki. Written informed consent was obtained from each patient included by the original institutions.

References

1. Sung H, Ferlay J, Siegel RL, Laversanne M, Soerjomataram I, Jemal A, et al. Global Cancer statistics 2020: GLOBOCAN estimates of incidence and Mortality Worldwide for 36 cancers in 185 countries. CA Cancer J Clin. 2021;71:209–49. doi: 10.3322/caac.21660
2. Kennecke H, Yerushalmi R, Woods R, Cheang MCU, Voduc D, Speers CH, et al. Metastatic behavior of Breast cancer subtypes. J Clin Oncol. 2010;28:3271–7. doi: 10.1200/JCO.2009.25.9820
3. Ensenyat-Mendez M, Llinàs-Arias P, Orozco JIJ, Íñiguez-Muñoz S, Salomon MP, Sesé B et al. Current triple-negative Breast Cancer subtypes: dissecting the most aggressive form of Breast Cancer. Front Oncol. 2021;2311
4. Dillekås H, Rogers MS, Straume O. Are 90% of deaths from Cancer caused by metastases? Cancer Med. 2019;8:5574–6. doi: 10.1002/cam4.2474
5. Lesurf R, Aure MR, Mørk HH, Vitelli V, Oslo Breast Cancer Research Consortium (OSBREAC) Lundgren S, et al. Molecular features of subtype-specific progression from Ductal Carcinoma in situ to invasive Breast Cancer. Cell Rep. 2016;16:1166–79. doi: 10.1016/j.celrep.2016.06.051
6. van Seijen M, Lips EH, Thompson AM, Nik-Zainal S, Futreal A, Hwang ES et al. Ductal carcinoma in situ: to treat or not to treat, that is the question. Br J Cancer. 2019;121:285–92
7. Cui N, Hu M, Khalil RA. Biochemical and biological attributes of Matrix metalloproteinases. Prog Mol Biol Transl Sci. 2017;147:1–73. doi: 10.1016/bs.pmbts.2017.02.005
8. Cox TR. The matrix in cancer. Nat Rev Cancer. 2021;21:217–38. doi: 10.1038/s41568-020-00329-7
9. Cabral-Pacheco GA, Garza-Veloz I, Rosa CC-D, la, Ramirez-Acuna JM, Perez-Romero BA, Guerrero-Rodriguez JF, et al. The roles of matrix metalloproteinases and their inhibitors in human Diseases. Int J Mol Sci. 2020;21:9739. doi: 10.3390/ijms21249739
10. Gobin E, Bagwell K, Wagner J, Mysona D, Sandirasegarane S, Smith N, et al. A pan-cancer perspective of matrix metalloproteases (MMP) gene expression profile and their diagnostic/prognostic potential. BMC Cancer. 2019;19:1–10. doi: 10.1186/s12885-019-5768-0
11. Owyong M, Chou J, Bijgaart RJE, van den, Kong N, Efe G, Maynard C et al. MMP9 modulates the metastatic cascade and immune landscape for Breast cancer anti-metastatic therapy. Life Sci Alliance. 2019;2
12. Wang Q-M, Lv L, Tang Y, Zhang L, Wang L-F. MMP–1 is overexpressed in triple–negative Breast cancer tissues and the knockdown of MMP–1 expression inhibits Tumor cell malignant behaviors in vitro. Oncol Lett. 2019;17:1732–40. doi: 10.3892/ol.2018.9779
13. Jiang H, Li H. Prognostic values of tumoral MMP2 and MMP9 overexpression in Breast cancer: a systematic review and meta-analysis. BMC Cancer. 2021;21:1–13. doi: 10.1186/s12885-021-07860-2
14. Decock J, Hendrickx W, Vanleeuw U, Belle VV, Huffel SV, Christiaens M-R, et al. Plasma MMP1 and MMP8 expression in Breast cancer: protective role of MMP8 against lymph node Metastasis. BMC Cancer. 2008;8:1–8. doi: 10.1186/1471-2407-8-77
15. Juurikka K, Butler GS, Salo T, Nyberg P, Åström P. The role of MMP8 in cancer: a systematic review.

Int J Mol Sci. 2019;20:4506. doi: 10.3390/ijms20184506
16. Gutiérrez-Fernández A, Fueyo A, Folgueras AR, Garabaya C, Pennington CJ, Pilgrim S, et al. Matrix metalloproteinase-8 functions as a Metastasis suppressor through modulation of Tumor cell adhesion and invasion. Cancer Res. 2008;68:2755–63. doi: 10.1158/0008-5472.CAN-07-5154
17. Noël A, Gutiérrez-Fernández A, Sounni NE, Behrendt N, Maquoi E, Lund IK, et al. New and paradoxical roles of matrix metalloproteinases in the Tumor microenvironment. Front Pharmacol. 2012;3:140. doi: 10.3389/fphar.2012.00140
18. Chernov AV, Strongin AY. Epigenetic regulation of matrix metalloproteinases and their collagen substrates in cancer. Biomol Concepts. 2011;2(3):135–47
19. 19.Sato N, Maehara N, Su GH, Goggins M. Effects of 5-aza-2′-deoxycytidine on matrix metalloproteinase expression and Pancreatic cancer cell invasiveness. J Natl Cancer Inst. 2003;95:327–30. doi: 10.1093/jnci/95.4.327
20. Klassen LMB, Chequin A, Manica GCM, Biembengut IV, Toledo MB, Baura VA, et al. MMP9 gene expression regulation by intragenic epigenetic modifications in Breast cancer. Gene. 2018;642:461–6. doi: 10.1016/j.gene.2017.11.054.
21. Allison KH, Hammond MEH, Dowsett M, McKernin SE, Carey LA, Fitzgibbons PL, et al. Estrogen and progesterone receptor testing in Breast Cancer: ASCO/CAP Guideline Update. J Clin Oncol off J Am Soc Clin Oncol. 2020;38:1346–66. doi: 10.1200/JCO.19.02309
22. Wolff AC, Hammond MEH, Allison KH, Harvey BE, Mangu PB, Bartlett JMS, et al. Human epidermal growth factor receptor 2 testing in Breast Cancer: American Society of Clinical Oncology/College of American Pathologists Clinical Practice Guideline Focused Update. J Clin Oncol off J Am Soc Clin Oncol. 2018;36:2105–22. doi: 10.1200/JCO.2018.77.8738
23. Aran D, Sirota M, Butte AJ. Systematic pan-cancer analysis of tumour purity. Nat Commun. 2015;6:8971. doi: 10.1038/ncomms9971
24. Li D, Purushotham D, Harrison JK, Hsu S, Zhuo X, Fan C, et al. WashU Epigenome Browser update 2022. Nucleic Acids Res. 2022;50:W774–781. doi: 10.1093/nar/gkac238
25. Lánczky A, Győrffy B. Web-based Survival Analysis Tool tailored for Medical Research (KMplot): development and implementation. J Med Internet Res. 2021;23:e27633. doi: 10.2196/27633
26. GTEx Consortium The genotype-tissue expression (GTEx) project. Nat Genet. 2013;45:580–5. doi: 10.1038/ng.2653
27. Ghandi M, Huang FW, Jané-Valbuena J, Kryukov GV, Lo CC, McDonald ER, et al. Next-generation characterization of the Cancer Cell Line Encyclopedia. Nature. 2019;569:503–8. doi: 10.1038/s41586-019-1186-3
28. ICGC/TCGA Pan-Cancer Analysis of Whole Genomes Consortium Pan-cancer analysis of whole genomes. Nature. 2020;578:82–93. doi: 10.1038/s41586-020-1969-6
29. Staaf J, Glodzik D, Bosch A, Vallon-Christersson J, Reuterswärd C, Häkkinen J, et al. Whole-genome sequencing of triple-negative breast cancers in a population-based clinical study. Nat Med. 2019;25:1526–33. doi: 10.1038/s41591-019-0582-4
30. Saal LH, Vallon-Christersson J, Häkkinen J, Hegardt C, Grabau D, Winter C, et al. The Sweden Cancerome Analysis network-breast (SCAN-B) Initiative: a large-scale multicenter infrastructure towards implementation of Breast cancer genomic analyses in the clinical routine. Genome Med. 2015;7:1–12. doi: 10.1186/s13073-015-0131-9
31. Staaf J, Häkkinen J, Hegardt C, Saal LH, Kimbung S, Hedenfalk I et al. RNA sequencing-based single sample predictors of molecular subtype and risk of recurrence for clinical assessment of early-stage breast cancer. Npj Breast Cancer. 2022;8:1–17.
32. Strand SH, Rivero-Gutiérrez B, Houlahan KE, Seoane JA, King LM, Risom T et al. Molecular classification and biomarkers of clinical outcome in breast ductal carcinoma in situ: analysis of TBCRC 038 and RAHBT cohorts. Cancer Cell. 2022;40:1521–1536.e7
33. Aran D, Hu Z, Butte AJ. xCell: digitally portraying the tissue cellular heterogeneity landscape. Genome Biol. 2017;18:1–14. doi: 10.1186/s13059-017-1349-1
34. Chen D, Lei EP. Function and regulation of chromatin insulators in dynamic genome organization. Curr Opin Cell Biol. 2019;58:61–8. doi: 10.1016/j.ceb.2019.02.001
35. de Wit E, Vos ESM, Holwerda SJB, Valdes-Quezada C, Verstegen MJAM, Teunissen H, et al.

CTCF binding polarity determines chromatin looping. Mol Cell. 2015;60:676–84. doi: 10.1016/j.molcel.2015.09.023

36. Gong Y, Ji P, Yang Y-S, Xie S, Yu T-J, Xiao Y et al. Metabolic-Pathway-Based Subtyping of Triple-Negative Breast Cancer Reveals Potential Therapeutic Targets. Cell Metab. 2021;33:51–64.e9.
37. Majidpoor J, Mortezaee K. Steps in Metastasis: an updated review. Med Oncol Northwood Lond Engl. 2021;38:3. doi: 10.1007/s12032-020-01447-w
38. Roberti MP, Arriaga JM, Bianchini M, Quintá HR, Bravo AI, Levy EM, et al. Protein expression changes during human triple negative Breast cancer cell line progression to lymph node Metastasis in a xenografted model in nude mice. Cancer Biol Ther. 2012;13:1123–40. doi: 10.4161/cbt.21187
39. Zhu Y, Tao Z, Chen Y, Lin S, Zhu M, Ji W, et al. Exosomal MMP-1 transfers Metastasis potential in triple-negative Breast cancer through PAR1-mediated EMT. Breast Cancer Res Treat. 2022;193:65–81. doi: 10.1007/s10549-022-06514-6
40. Si W, Xu X, Wan L, Lv F, Wei W, Xu X et al. RUNX2 facilitates aggressiveness and chemoresistance of triple negative breast cancer cells via activating MMP1. Front Oncol. 2022;12.
41. Lim JP, Nair S, Shyamasundar S, Chua PJ, Muniasamy U, Matsumoto K, et al. Silencing Y-box binding protein-1 inhibits triple-negative Breast cancer cell invasiveness via regulation of MMP1 and beta-catenin expression. Cancer Lett. 2019;452:119–31. doi: 10.1016/j.canlet.2019.03.014
42. Thirkettle S, Decock J, Arnold H, Pennington CJ, Jaworski DM, Edwards DR. Matrix metalloproteinase 8 (collagenase 2) induces the expression of interleukins 6 and 8 in Breast cancer cells. J Biol Chem. 2013;288:16282–94. doi: 10.1074/jbc.M113.464230
43. Decock J, Hendrickx W, Thirkettle S, Gutiérrez-Fernández A, Robinson SD, Edwards DR. Pleiotropic functions of the tumor- and metastasis-suppressing matrix metalloproteinase-8 in mammary cancer in MMTV-PyMT transgenic mice. Breast Cancer Res BCR. 2015;17:38. doi: 10.1186/s13058-015-0545-8
44. 44.Soria-Valles C, Gutiérrez-Fernández A, Guiu M, Mari B, Fueyo A, Gomis RR, et al. The anti-metastatic activity of collagenase-2 in Breast cancer cells is mediated by a signaling pathway involving decorin and miR-21. Oncogene. 2014;33:3054–63. doi: 10.1038/onc.2013.267
45. 45.Sarper M, Allen MD, Gomm J, Haywood L, Decock J, Thirkettle S, et al. Loss of MMP-8 in ductal carcinoma in situ (DCIS)-associated myoepithelial cells contributes to tumour promotion through altered adhesive and proteolytic function. Breast Cancer Res BCR. 2017;19:33. doi: 10.1186/s13058-017-0822-9
46. 46.González LO, González-Reyes S, Junquera S, Marín L, González L, Del Casar JM, et al. Expression of metalloproteases and their inhibitors by Tumor and stromal cells in ductal carcinoma in situ of the breast and their relationship with microinvasive events. J Cancer Res Clin Oncol. 2010;136:1313–21. doi: 10.1007/s00432-010-0782-2
47. 47.Rao SSP, Huntley MH, Durand NC, Stamenova EK, Bochkov ID, Robinson JT, et al. A 3D map of the human genome at kilobase resolution reveals principles of chromatin looping. Cell. 2014;159:1665–80. doi: 10.1016/j.cell.2014.11.021
48. 48.Flavahan WA, Drier Y, Liau BB, Gillespie SM, Venteicher AS, Stemmer-Rachamimov AO, et al. Insulator dysfunction and oncogene activation in IDH mutant gliomas. Nature. 2016;529:110–4. doi: 10.1038/nature16490
49. 49.Guo Y, Xu Q, Canzio D, Shou J, Li J, Gorkin DU, et al. CRISPR Inversion of CTCF Sites Alters Genome Topology and Enhancer/Promoter function. Cell. 2015;162:900–10. doi: 10.1016/j.cell.2015.07.038
50. 50.Liu EM, Martinez-Fundichely A, Diaz BJ, Aronson B, Cuykendall T, MacKay M, et al. Identification of Cancer drivers at CTCF insulators in 1,962 whole genomes. Cell Syst. 2019;8:446–455e8. doi: 10.1016/j.cels.2019.04.001
51. 51.Nuñez-Olvera SI, Puente-Rivera J, Ramos-Payán R, Pérez-Plasencia C, Salinas-Vera YM, Aguilar-Arnal L, et al. Three-Dimensional Genome Organization in breast and gynecological cancers: how chromatin folding influences Tumorigenic Transcriptional Programs. Cells. 2021;11:75. doi: 10.3390/cells11010075
52. 52.Liu F, Wu D, Wang X. Roles of CTCF in conformation and functions of chromosome. Semin Cell Dev Biol. 2019;90.